

# Strain-dependent optical properties in Janus MoSSe monolayer



Yi-Syun Hsieh<sup>1,2\*</sup>, Hao-Yu Cheng<sup>1</sup>, Tzu-Hsuan Weng<sup>1</sup>, Tianyi Zhang<sup>3</sup>, Jing Kong<sup>3</sup>, and Kung-Hsuan Lin<sup>1</sup>

<sup>1</sup> Institute of Physics, Academia Sinica, Taipei 11529, Taiwan

<sup>2</sup> Department of Physics, National Dong Hwa University, Hualien 974301, Taiwan

<sup>3</sup> Department of Electrical Engineering & Computer Science, Massachusetts Institute of Technology, Cambridge, MA 02138, USA

## Abstract

Janus transition metal dichalcogenides (TMDs) with engineered broken mirror symmetry provide a versatile nonlinear-optical platform with broadband tunability in harmonic generation [1]. Here, we investigate the strain-dependent photoluminescence (PL) and angle-resolved second-harmonic generation (SHG) responses of a Janus MoSSe monolayer under uniaxial compressive strain. In addition, first-principles calculations are performed to study the electronic band structure as well as the strain dependence of the SHG susceptibility and anisotropic SHG patterns. In our PL measurements, uniaxial compressive strain applied along either the armchair or zigzag direction induces a blueshift in the emission energy, consistent with our band-structure calculations. In contrast, our SHG measurements show that the SHG intensity decreases with increasing compressive strain.

## Introduction

Janus TMD MoSSe hosts long-lived dipolar excitons [1] and exhibits superior electron mobility [2] as well as enhanced nonlinear optical responses [3]. These properties make Janus TMDs highly promising for applications in device fabrication and flexible electronics. Therefore, a fundamental understanding of the strain-dependent properties of MoSSe monolayers is crucial for the development of flexible devices.

## Principle

In second harmonic generation (SHG), the induced polarization arises from the second-order nonlinear susceptibility and is proportional to the square of the applied electric field. Since SHG is allowed only in non-centrosymmetric materials, it provides a powerful tool for determining crystal orientation.

$$P_i \propto \sum_{jk} \chi_{ijk}^{(2)} E_j E_k$$

$$\begin{pmatrix} P_x^{(2)} \\ P_y^{(2)} \\ P_z^{(2)} \end{pmatrix} \propto \begin{pmatrix} 0 & 0 & 0 & 0 & d_{15} & -d_{22} \\ -d_{22} & d_{22} & 0 & d_{15} & 0 & 0 \\ d_{31} & d_{31} & d_{33} & 0 & 0 & 0 \end{pmatrix} \begin{pmatrix} \cos^2\theta \\ \sin^2\theta \\ 0 \\ 0 \\ 0 \\ 0 \end{pmatrix} = \begin{pmatrix} -d_{22}\sin 2\theta \\ -d_{22}\cos 2\theta \\ d_{31} \end{pmatrix}$$

parallel SHG intensity  $I_{\parallel}(2\omega) \propto |\hat{E}_{2\omega} P(2\omega)|^2 = |d_{22}\sin 3\theta|^2$

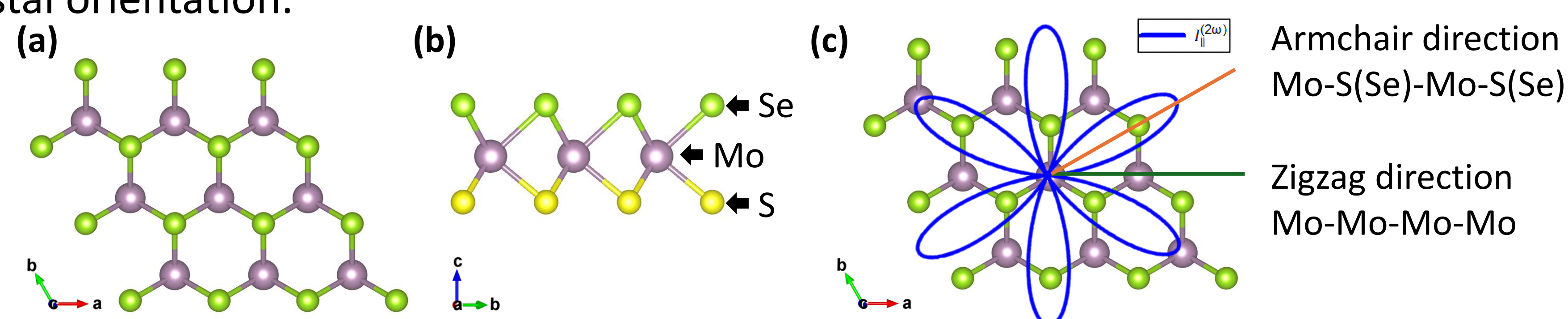


Fig.1. Crystal structure of the Janus MoSSe monolayer: (a) top view; (b) side view; (c) atomic species legend. (The blue line depicts the intensity of the SHG signal with polarization parallel to the incident light, denoted as  $I_{\parallel}(2\omega)$ )

## First-principles calculations

The first-principles method used to calculate the band structure based on density functional theory (DFT), generalized gradient approximations (GGA) with the Perdew-Burke-Ernzerhof (PBE) functional, which was used to describe the electron exchange correlation interactions [4].

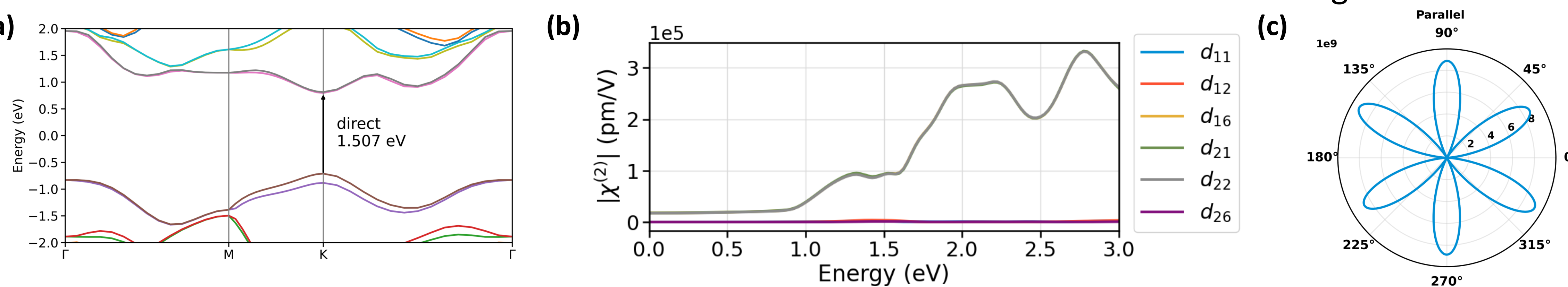
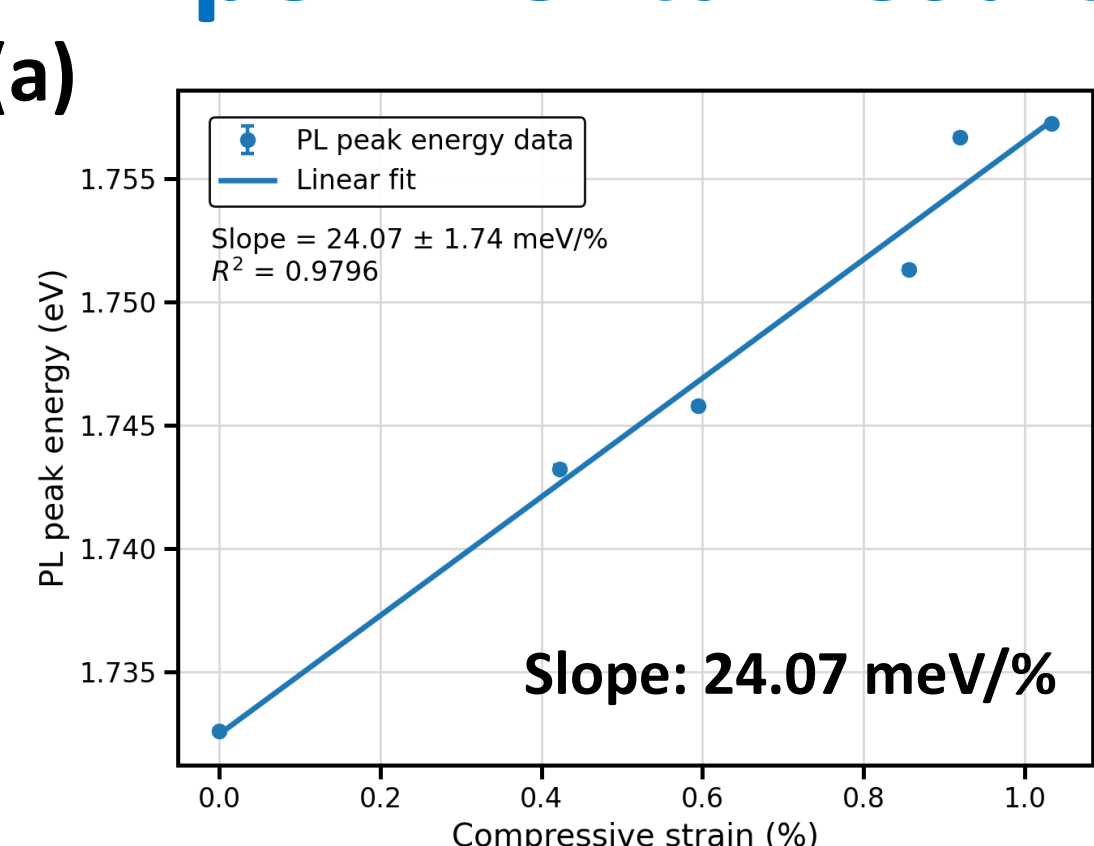


Fig.2. The DFT-calculated results of unstrained Janus MoSSe monolayer: (a) the band structure; (b) the absolute values of SHG susceptibility components; (c) angle-resolved SHG polar pattern (parallel polarization)

## Results Part I: Strain-dependent PL peak shifts

Applied compressive strain on crystal **armchair** direction

### Experimental results



### Simulation results

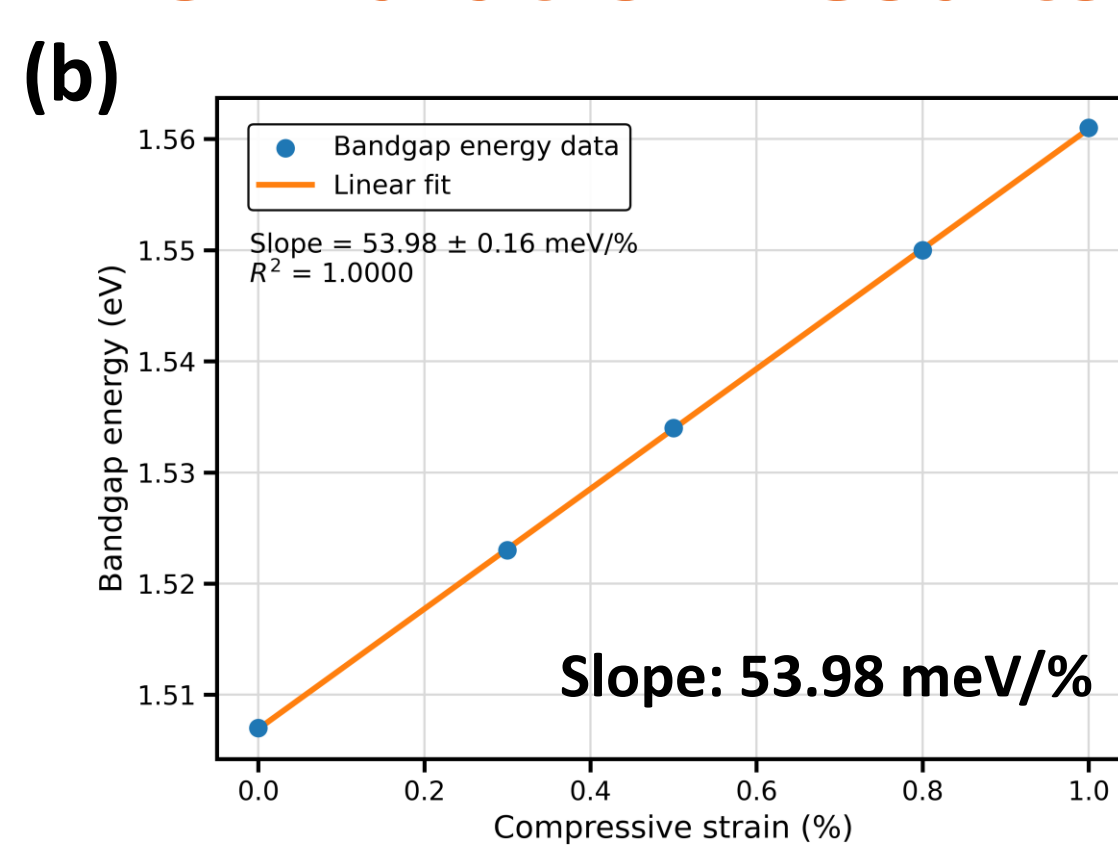


Fig. 3. Energy shifts in monolayer MoSSe under compressive strain along the crystal armchair direction: (a) PL peak energy with linear fitting; (b) DFT-calculated bandgap energy with linear fitting.

Applied compressive strain on crystal **zigzag** direction

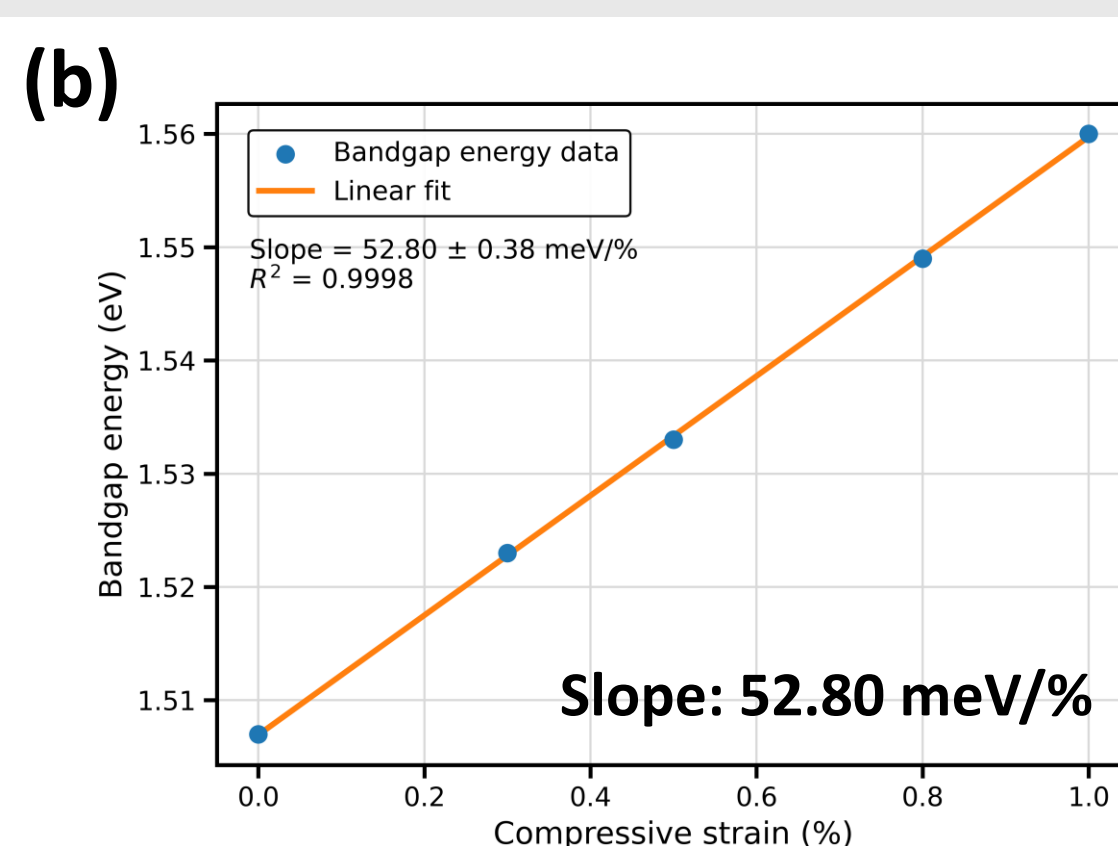
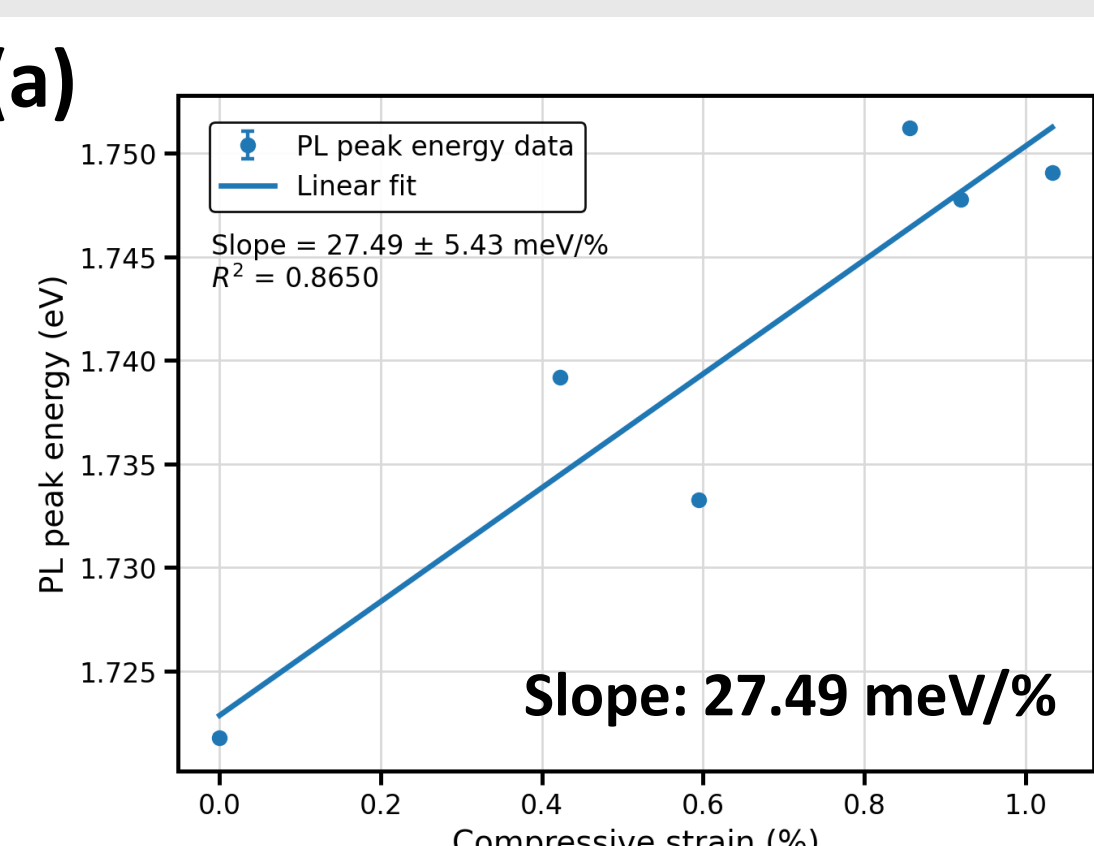
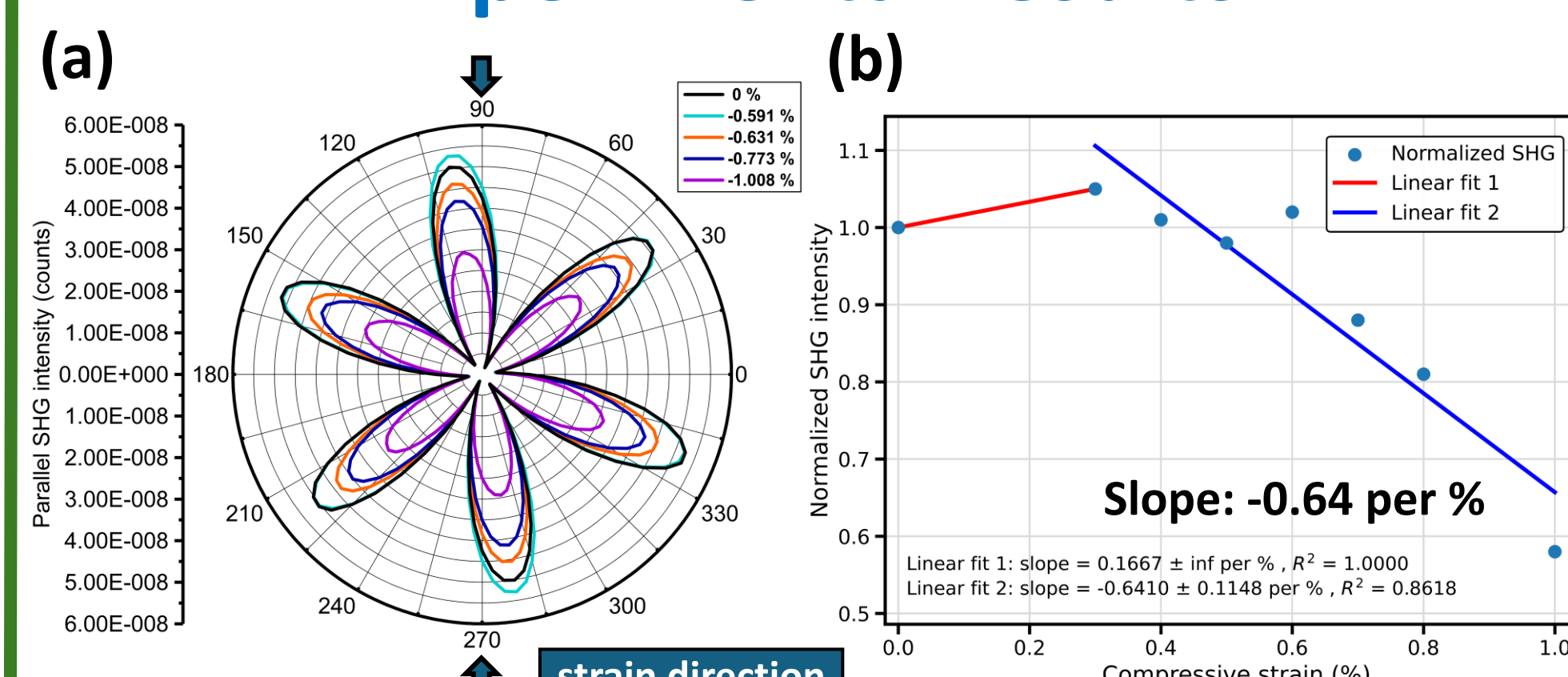


Fig. 4. Energy shifts in monolayer MoSSe under compressive strain along the crystal zigzag direction: (a) PL peak energy with linear fitting; (b) DFT-calculated bandgap energy with linear fitting.

## Part II: Strain-dependent angle-resolved parallel SHG intensity

Applied compressive strain on crystal **armchair** direction

### Experimental results



### Simulation results

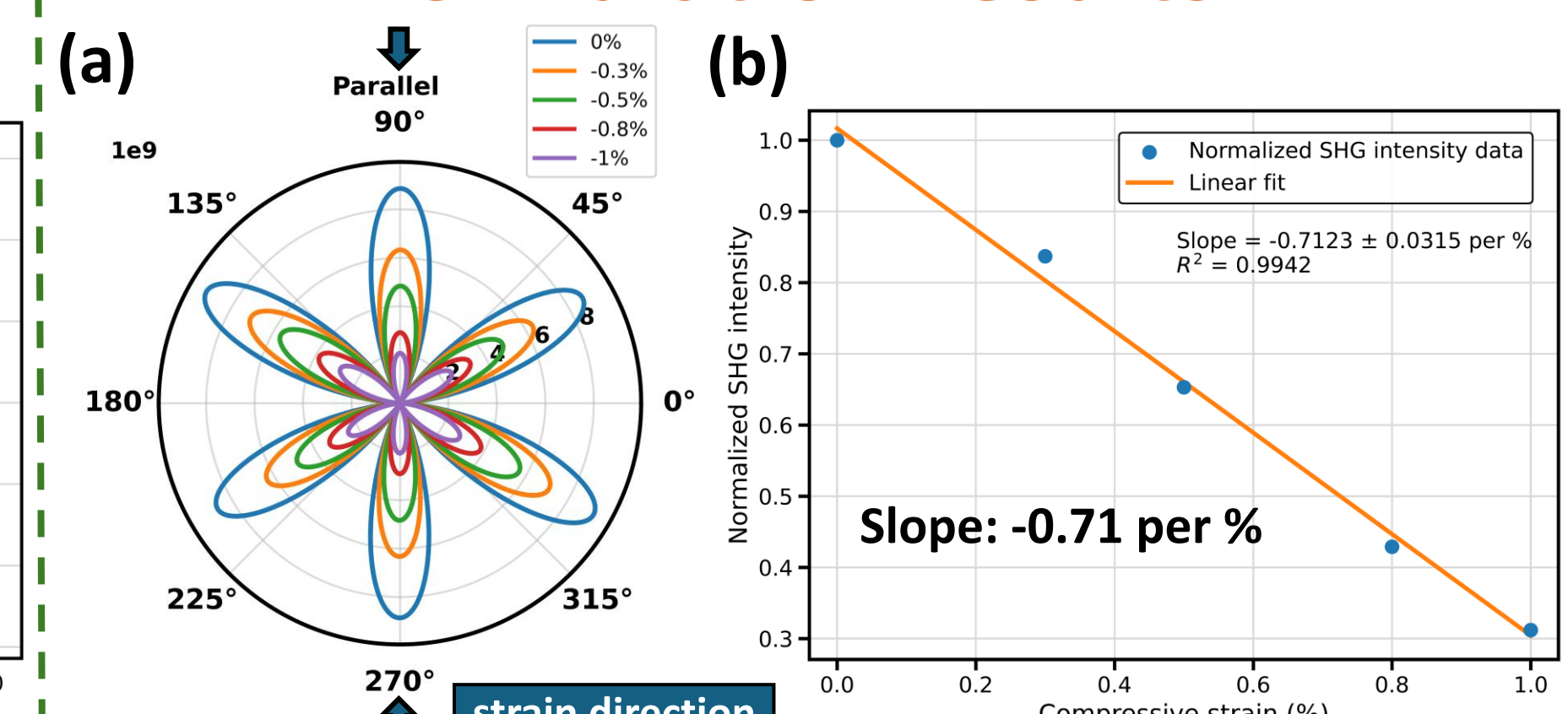


Fig. 5. Strain-dependent SHG under compressive strain along armchair direction: (a) angle-resolved parallel SHG intensity; (b) normalized SHG intensity.

Fig. 6. DFT-calculated strain-dependent SHG under compressive strain along the armchair direction: (a) angle-resolved parallel SHG; (b) normalized SHG.

Applied compressive strain on crystal **zigzag** direction

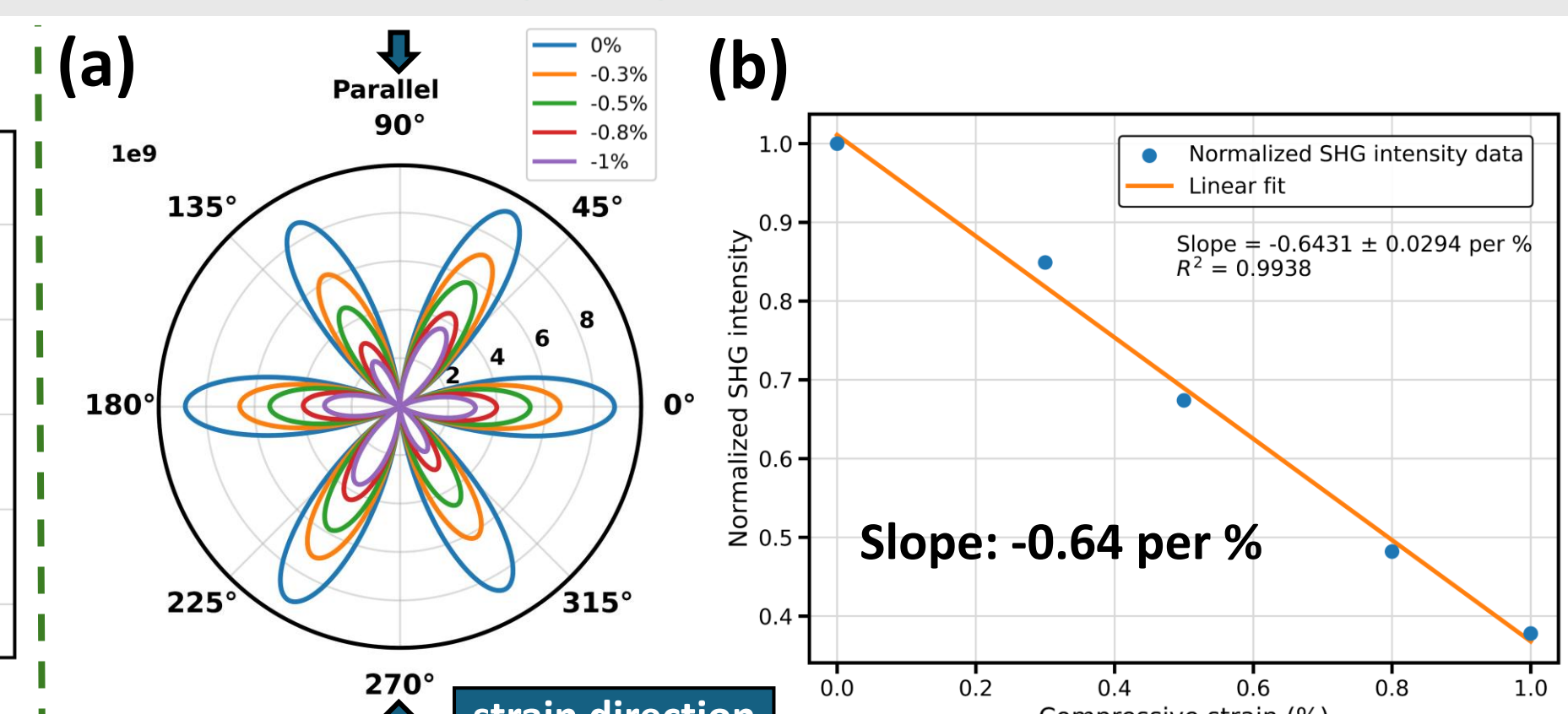
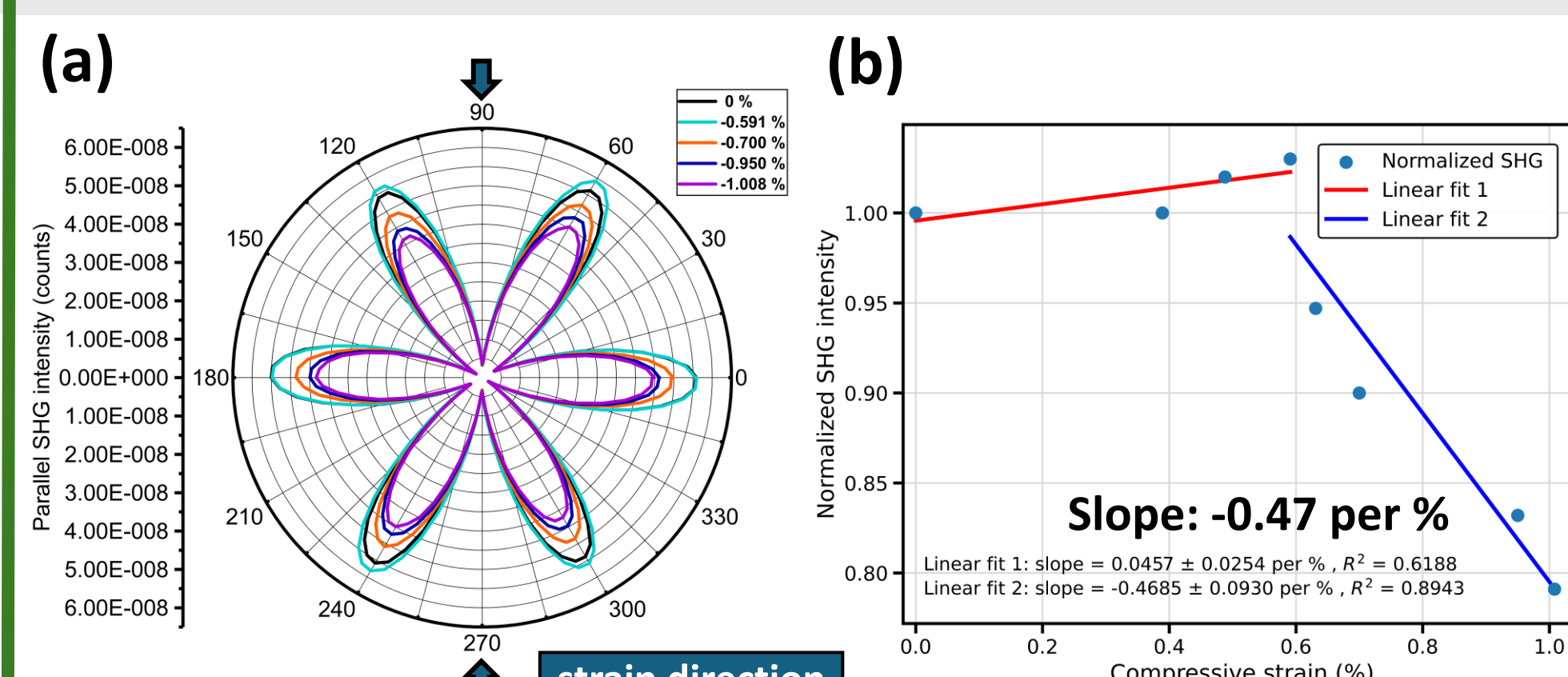


Fig. 7. Strain-dependent SHG under compressive strain along zigzag direction: (a) angle-resolved parallel SHG intensity; (b) normalized SHG intensity.

Fig. 8. DFT-calculated strain-dependent SHG under compressive strain along the zigzag direction: (a) angle-resolved parallel SHG; (b) normalized SHG.

## Conclusion

- In our PL measurements, applying compressive strain along either the armchair or the zigzag direction causes a blue shift in the emission energy, consistent with the band structure simulation results.
- In the experimental results, the SHG intensity of monolayer MoSSe decreases under uniaxial compressive strain, regardless of whether the strain is applied along the armchair or zigzag direction.

## Reference

- [1] Marko M. Petric, et al, *Advance Optical Materials*, 2023, 11, 19, 2300958
- [2] Nguyen N.Hieu, et al, *Chemical Physics*, 2024, 583, 112300
- [3] Hsiu-Chi Pai, Yuh-Renn Wu, *Journal of Applied Physics*, 2022, 131, 14
- [4] Wen-Jin Yin, et al, *Journal of Materials Chemistry C*, 2018, 6, 1693